ISSN 2347-3487

Molecular Spectroscopic Characterization and Electronic Structure Analysis of N- benzylaniline- A DFT Approach

T.Chithambarathanu *, K.Vanaja, J.DaisyMagdaline
Department of Physics, S.T.Hindu College, Nagercoil, India
tchithambarathanu@gmail.com
Department of Physics, Rani Anna Government Arts college for women, Tirunelveli, India
vanaja.ela@gmail.com
Department of Physics, Rani Anna Government Arts college for women, Tirunelveli, India
sugunajose@gmail.com

ABSTRACT

The FT-IR and FT-Raman spectra of N-benzylaniline[NBZA] have been analysed in the region 4000-450cm^{-1} and 4000-50cm^{-1}respectively. The geometrical structure, harmonic vibrational frequency, infrared intensity, Raman activities and bonding features of the title compound were carried out by DFT method with B3LYP/6-311++G(d, p) basis set. The complete vibrational frequency assignments were made by normal co-ordinate analysis following the scaled quantum mechanical force field methodology (SQM). The charge transfer and hyperconjugative interactions have been analysed using natural bond orbital (NBO) and HOMO-LUMO analysis. The reactivity sites are identified by mapping the electron density into electrostatic potential surface (MESP). The thermodynamic properties of the title compound at the different temperatures have been calculated. The mulliken charges, the values of electric dipole moment (μ) of the molecule were computed using DFT calculations and the results are interpreted. The UV absorption spectrum of the title compound has been described at the experimental level.

Keywords

N-benzylaniline; DFT; FT-IR; FT-Raman; NBO; UV.

Academic Discipline And Sub-Disciplines

Science(Physics)

SUBJECT CLASSIFICATION

Physics(Molecular Spectroscopy)

TYPE (METHOD/APPROACH)

Quasi-Experimental;

Council for Innovative Research
Peer Review Research Publishing System
Journal: JOURNAL OF ADVANCES IN PHYSICS
Vol.8, No.3
www.cirjap.com, japeditor@gmail.com

ISSN 2347-3487

1. INTRODUCTION

N-benzylaniline is an N- alkylated derivative of aniline. Aniline, a primary aromatic amine, is a weak base which forms salts with mineral acids. Aniline derivatives are widely used in pharmaceutical manufacturing, electro-optical, dye stuff and other commercial and industrial applications [1]. Some of the para substituted derivatives of aniline are commonly used as local anesthetics. Aniline and its derivatives are also important in the manufacture of rubber – processing chemicals and varnishes. Aniline derivatives such as phenylenediamines and diphenylamine are antioxidants. Fluoroanilines are important molecules in chemical industries for the synthesis of pigments, plastics and conducting polymers [2] and in the manufacture of agrochemicals [3]. Krishnakumaret al. [4] have studied the spectral analysis of 2, 6 - dibromo - 4 – nitroaniline and 2-(methylthio) aniline based on density functional theory. Sundaraganesanet al. [5] investigated the experimental vibrational spectra of 3, 4- dimethoxy aniline by using ab initio and DFT methods.

In this aniline series, N-benzylaniline acts as a protecting agent against cerebral ischemia injury and it has an analgestic action for chronic pathologic pains. It is used as a drug for cerebral apoplexy, neuropathic and inflammatory pain [6]. Owing to the industrial and biological importance, an extensive spectroscopic study on N- benzylaniline has been carried out in this present work. The molecular geometry and vibrational spectra of NBZA were calculated by applying the density functional theory (DFT) method with B3LYP functional at 6-311++G (d,p) basis set. A complete vibrational analysis of NBZA was performed by combining the experimental and theoretical information using Pulay's DFT based on the scaled quantum mechanical (SQM) approach. The redistribution of electron density (ED) in various bonding, antibonding orbitals and E(2) energies have been calculated by natural bond orbital (NBO) analysis to give clear evidence of stabilization originating from the hyper conjugation of various intra-molecular interactions. HOMO-LUMO analysis has been used to elucidate information regarding charge transfer within the molecule. The Molecular electrostatic potential (MEP), thermodynamic properties and Mulliken charge analysis have also been studied.

2. EXPERIMENTAL SECTION

The compound N-benzylaniline (NBZA) in the solid form was purchased from the Sigma Aldrich chemical company (USA) with a stated purity of 98% and used as such without further purification. FT-Raman spectra were recorded in the range of 4000-50cm^{-1} using BRUKER, Model RFS 100/s FT-Raman spectrophotometer. The FT-IR spectrum of the sample was recorded using Perkin Elmer RXI spectrometer in the region 4000-450cm^{-1} usingtheKBr pellet technique. UV-Vis absorption spectra were recorded in the polar solvents water and ethanol in the region 200-400 nm using Perkin Elmer LAMDA UV-vis NIR spectrometer. The polar solvents were used for the better stabilization of the exited state.

3. COMPUTATIONAL DETAILS

The DFT computation of NBZA had been performed using Gaussian 03 program package [7] at the Becke 3 – Lee – Yang – Parr (B3LYP) functional with the standard 6 - 3ll++G(d, p) basis set. The optimized structural parameters were evaluated for the calculations of vibrational frequencies at different methods. The harmonic vibrational frequencies had been analytically calculated by taking the second order derivative of energy using the same level of theory. The scaling of the force field was performed according to the scaled quantum mechanical procedure (SQM) [8, 9] using selective scaling in the natural internal co-ordinate representation [10, 11] to obtain a better agreement between the theory and the experiment. Normal co-ordinate analysis had been performed in order to obtain the detailed interpretation of the fundamental modes using the MOLVIB program version 7.0 written by Sundius [12, 13]. The Raman activities (S_i) calculated by the Gaussian 03W program and converted into relative Raman intensities (I_i) during the scaling program with MOLVIB using the following relationship derived from the basic theory of Raman scattering[14,15].

$$I_i = f(v_0 - v_i)^4 S_i v_i^{-1}[1-\exp(-hcv_i/Kt]^{-1} \quad (1)$$

The NBO calculations [16] were performed using NBO 3.1 program as carried out in the Gaussian 03 W package at the DFT/B3LYP level in order to understand the various second order interactions between the filled orbitals of one sub system and vacant orbitals of another sub system, which is a measure of delocalization or hyper conjugation. The all calculations presented in the work were also been carried out at the same level of theory of NBO calculations using 6-311++G (d, p) basis set.

4. RESULT AND DISCUSSION

4.1 Molecular Geometry

The optimized geometry performed at B3LYP/6-311++G (d,p) basis set of the title molecule is shown in Fig.1.with atom numbering scheme. The comparative optimized structural parameters such as bond lengths, bond angles along with its experimental data obtained by the X-ray analysis of NBZA [17] are presented in Table 1. All the optimized C-C bond lengths are larger than the experimental values, due to the fact that theoretical calculations belong to isolated molecules in the gaseous phase and the experimental results belong to the molecule in the solid state.

The C-C bond lengths in aniline and benzyl ring of the NBZA lie in the range 1.387-1.409 A^0 and 1.392-1.400 A^0 respectively by B3LYP/6-311++G(d, p) method ,but due to the substituent of NH_2 the bond lengths C2-C3(1.409A^0) and C2-C7(1.405A^0) in the aniline ring show a considerable increase . All the C-C bond lengths in the aniline ring and benzyl ring except C2-C3, C2-C7 are in agreement with literature values [18]. The bond length C8-C9 (1.513 A^0),which forms a bridge between the two ring systems, is found to be longer than that of the standard C-C bond length of about

ISSN 2347-3487

1.47 A^0[19]. In the title compound, the shortening of the C-N bond lengths C2-N1 (1.392 A^0) and C8-N1 (1.459 A^0) from the normal single bond length (1.48 A^0) reveals the effect of resonance [20] on that part of the molecule. But due to the coulomb repulsive interaction of methylene, an asymmetry is observed in C2-N1 and C8-N1 bond lengths.

With the electron donating substituent ($-C_7H_7$) on the aniline ring, the symmetry of the ring is distorted yielding ring angles C3-C2-C7 (118.243^0) and C4-C5-C6 (118.753^0) smaller than 120^0 at the point of substitution and the other angles C2-C3-C4(120.812), C3-C4-C5(120.747), C5-C6-C7(121.112) and C2-C7-C6(120.33) slightly larger than 120^0. This value is typical for aniline compounds such as m-methylaniline[21] and p-methylaniline[22]. The C10-C9-C14 (118.771^0) bond angle in benzyl ring is also smaller than the normal 120^0, which is due to the presence of aniline ring. At C2 position, the bond angles C3-C2-N1 and C7-C2-N1 are 119.322^0 and 122.41^0 respectively. This asymmetry in angles reveals the interaction between Nitrogen in the aniline and the benzene ring.

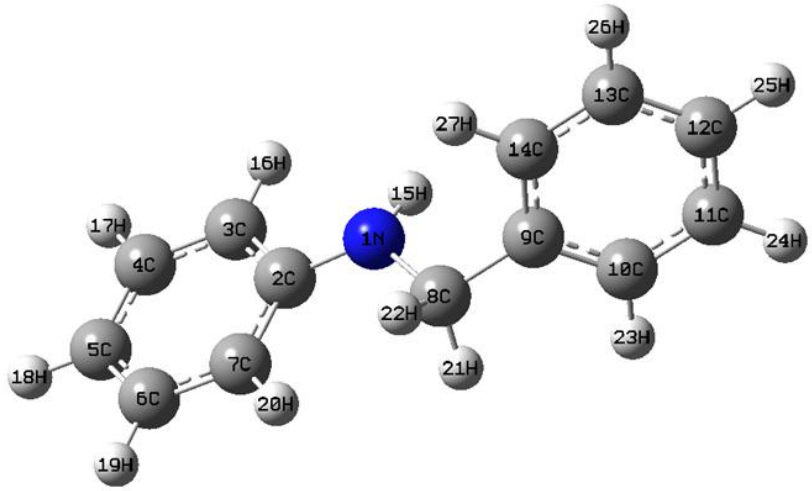

Fig.1 Molecular structure of N - benzylaniline along with numbering of atoms.

Table 1 : Experimental (XRD) and optimized geometrical parameters of N-benzylaniline obtained by B3LYP/6-311++G (d,p) method.

Bond length	Experimental value	B3LYP/6-311**G	Bond angle	Experimental value	B3LYP/6-311++G	Dihedral angle	B3LYP/6-311++G
N1-C2	1.375	1.392	C2-N1-C8	123.91	121.993	C8-N1-C2-C3	-165.9
N1-C8	1.433	1.459	C2-N1-H15	117.24	114.591	C8-N1-C2-C7	15.921
N1-H15	0.86	1.01	C8-N1-H15	117.03	113.909	H15-N1-C2-C3	-21.662
C2-C3	1.395	1.409	N1-C2-C3	122.75	119.322	H15-N1-C2-C7	160.158
C2-C7	1.394	1.405	N1-C2-C7	118.94	122.41	C2-N1-C8-C9	177.238
C3-C4	1.384	1.387	C3-C2-C7	118.3	118.243	C2-N1-C8-H21	54.782
C3-H16	0.95	1.086	C2-C3-C4	120.05	120.812	C2-N1-C8-H22	-62.736
C4-C5	1.375	1.397	C2-C3-H16	120	119.215	H15-N1-C8-C9	32.781

C4-H17	0.95	1.085	C4-C3-H16	119.94	119.971	H15-N1-C8-H21	-89.675
C5-C6	1.38	1.391	C3-C4-C5	121.34	120.747	H15-N1-C8-H22	152.807
C5-H18	1.05	1.083	C3-C4-H17	119.29	119.234	N1-C2-C3-C4	-177.9
C6-C7	1.3777	1.395	C5-C4-H17	119.37	120.018	N1-C2-C3-H16	1.667
C6-H19	0.949	1.085	C4-C5-C6	118.62	118.753	C7-C2-C3-C4	0.352
C7-H20	0.949	1.083	C4-C5-H18	120.67	120.587	C7-C2-C3-H16	179.923
C8-C9	1.514	1.513	C6-C5-H18	120.71	120.66	N1-C2-C7-C6	177.549
C8-H21	0.991	1.1	C5-C6-C7	121.02	121.112	N1-C2-C7-H20	-2.378
C8-H22	0.99	1.096	C5-C6-H19	119.54	119.945	C3-C2-C7-C6	-0.649
C9-C10	1.388	1.397	C7-C6-H19	119.44	118.942	C3-C2-C7-H20	179.424
C9-C14	1.385	1.4	C2-C7-C6	120.64	120.33	C2-C3-C4-C5	0.108
C10-C11	1.385	1.396	C2-C7-H20	119.66	120.402	C2-C3-C4-H17	-179.96
C10-H23	0.95	1.085	C6-C7-C20	119.7	119.269	H16-C3-C4-C5	-179.46
C11-C12	1.373	1.392	N1-C8-C9	117.05	110.758	H16-C3-C4-H17	0.475
C11-H24	0.951	1.084	N1-C8-H21	108.07	111.753	C3-C4-C5-C6	-0.273
C12-C13	1.377	1.396	N1-C8-H22	108	108.525	C3-C4-C5-H18	179.934
C12-H25	0.951	1.084	C9-C8-H21	108.03	109.556	H17-C4-C5-C6	179.794
C13-C14	1.382	1.392	C9-C8-H22	108.05	109.333	H17-C4-C5-H18	0
C13-H26	0.96	1.084	H21-C8-H22	107.25	106.807	C4-C5-C6-C7	-0.03
C14-H27	0.95	1.085	C8-C9-C10	122.06	120.824	C4-C5-C6-H19	-179.68
			C8-C9-C14	118.69	120.405	H18-C5-C6-C7	179.764
			C10-C9-C14	118.41	118.771	H18-C5-C6-H19	0.113
			C9-C10-C11	120.38	120.742	C5-C6-C7-C2	0.498
			C9-C10-H23	119.82	119.493	C5-C6-C7-H20	-179.57
			C11-C10-H23	119.8	119.765	H19-C6-C7-C2	-179.85

C10-C11-C12	120.64	120.034	H19-C6-C7-H20	0.081
C10-C11-H24	119.7	119.82	N1-C8-C9-C10	-114.54
C12-C11-H24	119.66	120.146	N1-C8-C9-C14	65.198
C11-C12-C13	119.49	119.677	H21-C8-C9-C10	9.183
C11-C12-H25	120.23	120.179	H21-C8-C9-C14	-171.08
C13-C12-H25	120.27	120.144	H22-C8-C9-C10	125.914
C12-C13-C14	120.03	120.155	H22-C8-C9-C14	-54.344
C12-C13-H26	120	120.022	C8-C9-C10-C11	179.994
C14-C13-H26	119.97	119.823	C8-C9-C10-C23	-0.161
C9-C14-C13	121.03	120.621	C14-C9-C10-C11	0.247
C9-C14-H27	119.47	119.35	C14-C9-C10-H23	-179.91
C13-C14-H27	119.49	120.029	C8-C9-C14-C13	-179.89
			C8-C9-C14-H27	0.041
			C10-C9-C14-C13	-0.14
			C10-C9-C14-H27	179.788
			C9-C10-C11-C12	-0.193
			C9-C10-C11-H24	179.864
			H23-C10-C11-C12	179.961
			H23-C10-C11-H24	0.018
			C10-C11-C12-C13	0.027
			C10-C11-C12-H25	179.958
			H24-C11-C12-C13	179.97
			H24-C11-C12-H25	-0.099
			C11-C12-C13-C14	0.079
			C11-C12-C13-H26	179.834

H25-C12-C13-C14	-179.85
H25-C12-C13-H26	-0.097
C12-C13-C14-C9	-0.022
C12-C13-C14-H27	-179.95
H26-C13-C14-C9	-179.78
H26-C13-C14-H27	0.295

4.2. Potential energy surface scan

The potential energy surface (PES) with the B3LYP/6-311++G(d,p) level of theoretical approximation is performed for the title molecule by varying the dihedral angle C8-N1-C2-C3 in steps of 0^0,10^0,20^0, ...,360^0 and the resultant minimum energy curve as a function of dihedral angle is shown in Fig. 2.The conformational energy profile shows two maxima near 140^0 and 320^0. The maximum energies are obtained at -558.100518 and -558.100524 Hartree for 140^0 and 320^0 dihedral angles respectively. It is clear from Fig. 2.that there are four local minima observed at 30^0, 180^0, 200^0 and 350^0(-558.109683,-558.109682,-558.109682,-558.109683) for τ(C8-N1-C2-C3).

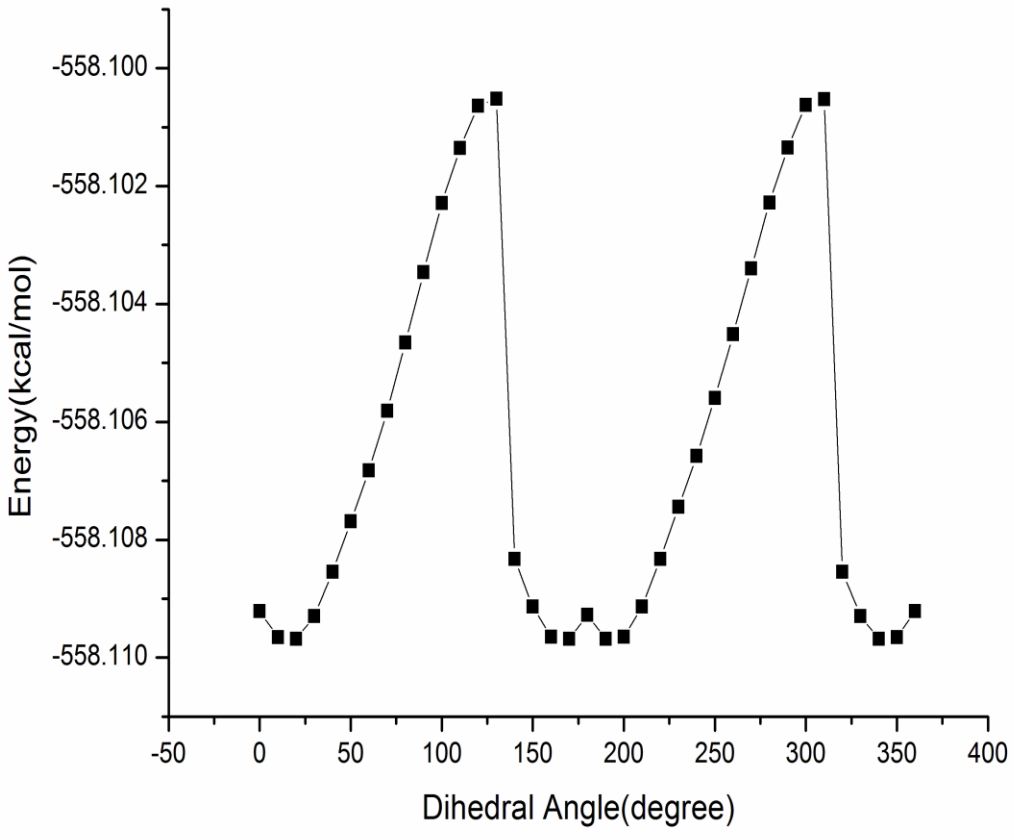

Fig .2. Potential energy surface of N-benzylaniline.

ISSN 2347-3487

4.3. Vibrational spectral analysis

The vibrational spectral assignments of NBZA have been carried out with the help of normal co-ordinate analysis. A non-redundant set of local symmetry co-ordinates are constructed by suitable linear combination of internal co-ordinates following the recommendations of Pulay et al.[8] are presented in Table 2. The computed wave numbers are selectively scaled according to the SQM procedure suggested by Rauhut and Pulay [8]. The observed and simulated FTIR and FT – Raman spectra of the compound are shown in Figs 3&4. The observed and calculated frequencies using B3LYP/6-311++G(d,p) basis set along with their relative intensities, probable assignments and potential energy distribution (PED) of NBZA are summarized in Table 3.

4.3.1. N-H Vibrations

The methylene and amino groups are generally referred to as electron donating substituents. In aromatic compounds, the associated N-H stretching vibration appears as moderate to strong band in the region 3410±70cm^{-1}[23]. For NBZA molecule, the N-H stretching mode is observed at 3415cm^{-1} in FT-IR as a strong band which agrees well with the computed wavenumber at 3415cm^{-1} by B3LYP/6-311++G(d, p) method with a PED contribution of 100%. The N-H in-plane and out of plane bending vibrations are expected in the range 1530±50cm^{-1}, 635±35cm^{-1} respectively [23]. In the title molecule, the strong broad band at 1489cm^{-1} in the FT-IR spectrum and a weak band in the FT-Raman spectrum at 1492cm^{-1}are assigned to N-H in plane bending modes. The N-H out of plane bending vibration is at 457cm^{-1} in FT-IR spectrum. The N-H in-plane and out of plane bending vibrations computed by B3LYP/6-311++G (d, p) method show good agreement with the recorded spectral data.

4.3.2. C-H Vibrations

In the aromatic compounds, the C-H stretching vibrations normally occur at 3100-3000cm^{-1} [24]. These vibrations are not found to be affected due to the nature and position of the substituent. In NBZA, the FT-IR bands at 3077, 3060, 3050 and 3025cm^{-1} and the FT-Raman bands at 3050 and 3025cm^{-1} are assigned to C-H stretching modes. The corresponding calculated wavenumbers at 3069, 3062, 3060, 3050, 3045, 3041, 3036, 3032, 3027 and 3024 cm^{-1} by B3LYP/6-311++G(d, p) level show good agreement with the observed bands of NBZA.

The aromatic C-H in-plane and out-of-plane bending vibrations occur in the range of 1390-1000cm^{-1} and 1000-720cm^{-1} in the substituted benzene compounds[25]. The experimental strong and medium FT-IR bands at 1321,1249, 1179, 1151, 1078 and 1065 cm^{-1} and the FT-Raman bands at1333,1319,1246, 1156, 1080 and 1065cm^{-1} are due to C-H in-plane bending. This observations agree well with the calculated values of the C-H in-plane bending vibrations at the B3LYP/6-311++G(d, p) level which lie in the range of 1313-1067 cm^{-1}.The frequencies of the C-H out of plane deformation vibrations are mainly determined by the number of adjacent hydrogen atoms on the ring[25]. The C-H out-of-plane bending vibrations calculated at 945 - 725cm^{-1}, show good agreement with the observed values of 794 and 727cm^{-1} in the FT-IR and 802cm^{-1}in the FT-Raman.

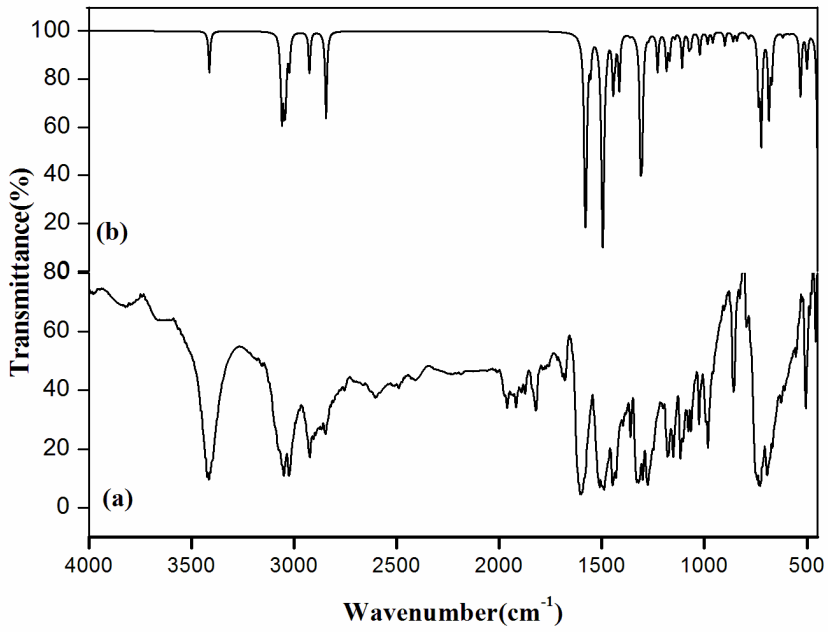

Fig.3 (a) Experimental and (b) Simulated Infrared spectra of N-benzylaniline

ISSN 2347-3487

4.3.3. C - C vibrations

The ring carbon – carbon stretching vibrations occur in the region 1250 – 1625cm^{-1}.In general, the C=C bands are of variable intensity and are observed at 1625 – 1590cm^{-1},1590 – 1575 cm^{-1} ,1525 – 1470cm^{-1} and 1465 – 1430cm^{-1}[25]. The C – C stretching vibrations of NBZA are observed at 1582, 1546 ,1431,1300 and 1026cm^{-1}in FT-IR spectrum and at 1582 , 1429,1302,1275 and 1028 cm^{-1}in FT Raman spectrum, which show good coherence with the theoretically calculated values 1582,1579,1565,1556,1479,1477,1437,1417,1306,1274,1025 and 1022cm^{-1} by B3LYP/6-311++G(d, p) method. For mono substituted aromatics, the bands due to the in-plane ring deformation vibration and out-of-plane ring deformation vibration appear in the region 830 – 435cm^{-1} and 710 – 405cm^{-1} respectively [23]. The in-plane ring deformation vibrations of NBZA are observed at 983,626,609 and 506cm^{-1} as strong and weak bands in the FT-IR and at 1000,987 and 617cm^{-1} in Raman spectrum. The out- of - plane ring deformation vibrations appear at 695 and 670 cm^{-1} in FT-IR spectrum and at 411cm^{-1}in Raman spectrum. The calculated bending modes found at 998,986,619,604,586,502 cm^{-1} and at 687,674,411 and 406cm^{-1}by B3LYP/6-311++G(d, p) method are assigned to C-C in-plane and out-of-plane ring deformation vibrations respectively.

4.3.4. C – N vibrations

The CN stretch, connected with the amine twist, appears as a moderate to strong band in the region 1075±25 cm^{-1}[23]. For NBZA , the strong CN stretching vibration band observed at 1117cm^{-1}both in FT-IR and FT-Raman agree well with the theoretically calculated frequency at 1110cm^{-1} by B3LYP/6-311++G(d,p) method. Primary aromatic amines (e-g anilines) have a weak to medium intensity band at 345-445cm^{-1}due to the C-N in-plane deformation. For mono substituted amino benzenes with electron donating substituents, this band is observed between 400-500cm^{-1}[25]. Accordingly, in the present study, the FT-Raman band assigned at 500cm^{-1}and FT-IR band assigned at 486cm^{-1}to C-N in-plane bending vibration of NBZA, which is in good agreement with the calculated value 501cm^{-1} by B3LYP/6-311++G (d, p) method.

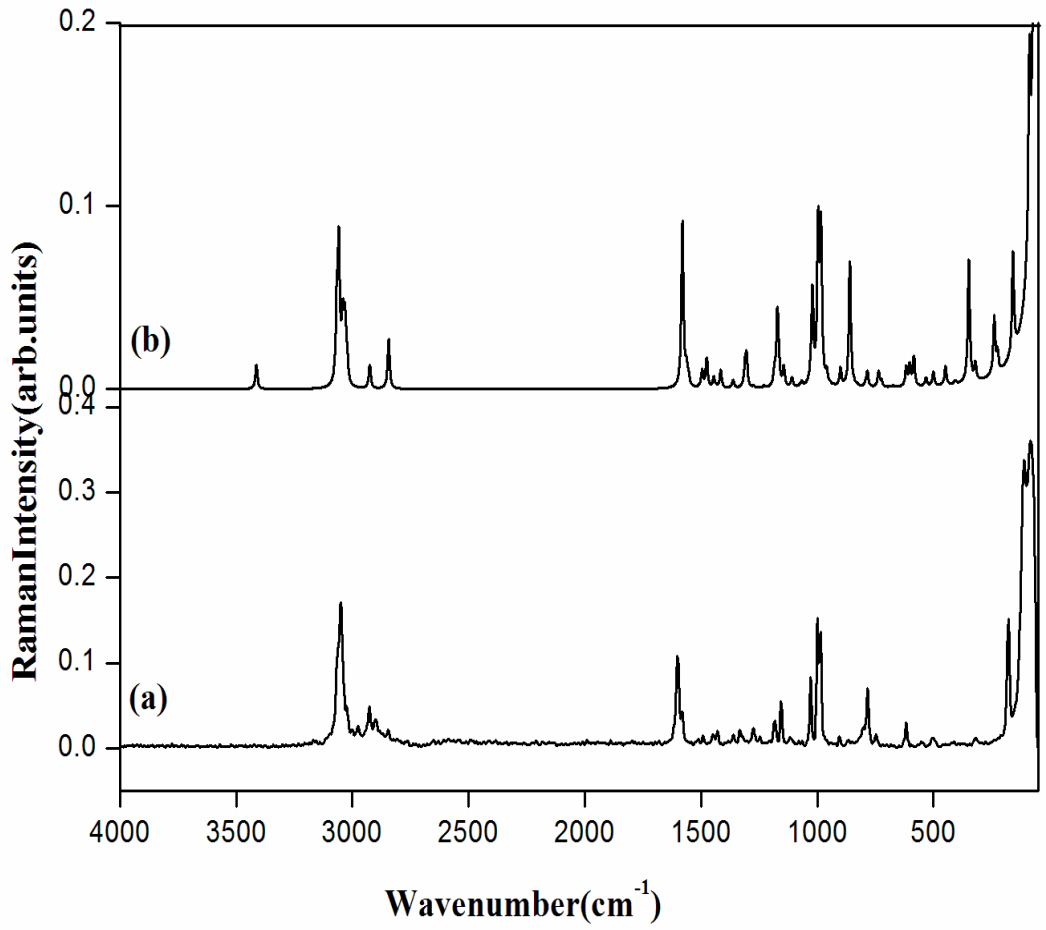

Fig 4 (a) Experimental and (b) simulated Raman Spectra of N-benzylaniline

4.3.5. Methylene group vibrations

The CH_2 group frequencies basically six fundamentals can be associated, namely, symmetric, asymmetric, scissoring, rocking, wagging and twisting vibrations. The methylene asymmetric stretching is found at 2930±15 cm^{-1} and the symmetric stretching at 2870 ±20 cm^{-1} [23]. In NBZA molecule, the computed wavenumbers at 2927 cm^{-1} and 2846 cm^{-1} by B3LYP/6-311++G(d, p) method are assigned to CH_2 asymmetric and symmetric stretching vibrations. In the present work, the strong band observed at 2923 cm^{-1} in the FT-IR and a medium band observed at 2927 cm^{-1} in the FT-Raman spectrum of NBZA are assigned to the CH_2 asymmetric modes of vibrations. Similarly, the band at 2846 cm^{-1} in the FT-IR and FT-Raman spectrum of NBZA is assigned to symmetric stretching mode of vibrations. The methylene deformation of $–CH_2NH_2$ compounds absorbs in the region 1450±20cm^{-1} with moderate intensity [23]. In title molecule, the δCH_2 vibration is observed at 1447 cm-1 as a strong band in the FT-IR and at 1447cm^{-1} as weak band in the FT-Raman spectrum. This agrees well with the computed wavenumbers at 1447 cm^{-1} by B3LYP/6-311++G(d, p) method. The methylene wag appears with a weak to moderate intensity in the region 1360±25 cm^{-1}[23]. For NBZA molecule, the wagging mode of CH_2 is observed at 1360cm^{-1} as a medium band in FT-IR and at 1361 cm^{-1} as weak band in the FT-Raman spectrum. The theoretically computed CH_2 wagging vibration at 1363 cm^{-1} by B3LYP/6-311++G (d,p) level shows good agreement with experimental results. The weak to moderate band at 1290±45 cm^{-1} is mostly assigned to the methylene twist [23]. The CH_2 twisting vibration of NBZA is observed at 1183cm^{-1} as a weak band in the FT-Raman spectrum. The computed wavenumber for the twisting mode is assigned at 1186 $cm^{-1}$by B3LYP/6-311++G (d, p) method. The methylene rocking vibrationsare observed in the region 890±55 cm^{-1} with band intensities varying from weak tomoderate [23]. The CH_2 rocking vibration of NBZA is attributed to 960 cm^{-1} in the FT-IR spectrum. The corresponding calculated wavenumber is at 960 cm^{-1} using B3LYP/6-311++G (d, p) basis set.

Table 2: Definition of local symmetry coordinates of NBZA

Sl No	Symmetry Coordinates	Description
1	S1= r2 7	υC2C7
2	S2= r7 6	υC7C6
3	S3= r6 5	υC6C5
4	S4= r5 4	υC5C4
5	S5= r4 3	υC4C3
6	S6= r3 2	υC3C2
7	S7= r12 11	υC12C11
8	S8= r11 10	υC11C10
9	S9= r10 9	υC10 C9
10	S10= r9 14	υC9C14
11	S11= r14 13	υC14C13
12	S12= r13 12	υC13C12
13	S13= r9 8	υC9C8
14	S14= r7 20	υC7H20
15	S15= r6 19	υC6H19
16	S16= r5 18	υC5H18
17	S17= r4 17	υC4H17

ISSN 2347-3487

18	S18= r3 16	υC3H16
19	S19= r10 23	υC10H23
20	S20= r11 24	υC11H24
21	S21= r12 25	υC12H25
22	S22= r13 26	υC13H26
23	S23= r14 27	υC14H27
24	S24= r2 1	υC2N1
25	S25= r8 1	υC8N1
26	S26= r1 15	υN1H15
27	S27=r 8 22+r 8 21	νCH2SS
28	S28= r 8 22 – r 8 21	νCH2AS
29	S29= β2 7 20 – β6 7 20	βC7H20
30	S30= β7 6 19 – β5 6 19	βC6H19
31	S31= β6 5 18 – β4 5 18	βC5H18
32	S32= β5 4 17 – β3 4 17	βC4H17
33	S33= β4 3 16 – β2 3 16	βC3H16
34	S34= β12 11 24 – β10 11 24	βC11H24
35	S35= β11 10 23 – β9 10 23	βC10H23
36	S36= β9 14 27 –β13 14 27	βC14H27
37	S37= β14 13 26 – β 12 13 26	βC13H26
38	S38= β13 12 25 – β11 12 25	βC12H25
39	S39= β7 2 1 – β3 2 1	βC2N1
40	S40= β8 1 15– β2 1 15	βN1H15
41	S41= β10 9 8 – β14 9 8	βC9C8
42	S42= β4 3 2 – β3 2 7 + β 2 7 6 – β7 6 5 + β6 5 4 – β 5 4 3	βring 1
43	S43= 2 β4 3 2 –β3 2 7 – β2 7 6+2 β7 6 5 – β6 5 4 – β5 4 3	βring 2
44	S44= β3 2 7 – β2 7 6 + β6 5 4 –β5 4 3	βring 3
45	S45= β14 13 12 – β13 12 11 + β12 11 10 – β11 10 9 + β10 9 14 – β9 14 13	βring 4
46	S46= 2 β14 13 12 – β13 12 11+ β12 11 10 +2 β11 10 9 – β10 9 14 – β9 14 13	βring 5
47	S47= β13 12 11 – β12 11 10 + β10 9 14 – β9 14 13	βring 6

48	S48 = 2 β8 1 2 – β2 1 15 – β8 1 15	δCNC
49	S49= 5 β9 8 1 + β22 8 21	δCCN
50	S50= 5 β22 8 21 + β9 8 1	CH2sc
51	S51 = β1 8 22+ β1 8 21– β9 8 22- β9 8 21	CH2wag
52	S52= β1 8 22- β1 8 21+ β9 8 22- β9 8 21	CH2ro
53	S53= β1 8 22- β9 8 22–β1 8 21+ β9 8 21	CH2twi
54	S54 = γ2 6 7 20	γ C7H20
55	S55 = γ7 5 6 19	γ C6H19
56	S56= γ4 6 5 18	γ C5H18
57	S57= γ3 5 4 17	γ C4H17
58	S58= γ2 4 3 16	γ C3H16
59	S59= γ12 10 11 24	γ C11H24
60	S60= γ11 9 10 23	γ C10H23
61	S61= γ13 9 14 27	γ C14H27
62	S62= γ12 14 13 26	γ C13H26
63	S63= γ11 13 12 25	γ C12H25
64	S64= γ3 7 2 1	γ C2N1
65	S65= γ8 9 10 14	γ C10C14
66	S66= γ8 2 1 15	γ N1H15
67	S67=τ4 3 2 7 – τ3 2 7 6 + τ2 7 6 5 – τ7 6 5 4 + τ6 5 4 3 – τ5 4 3 2	τring 1
68	S68= 2τ4 3 2 7 – τ3 2 7 6 – τ2 7 6 5+2 τ7 6 5 4 – τ6 5 4 3 – τ5 4 3 2	τring 2
69	S69=τ3 2 7 6 – τ2 7 6 5 + τ6 5 4 3 – τ5 4 3 2	τring 3
70	S70=τ14 13 12 11 – τ1312 11 10 + τ12 11 10 9 – τ11 10 9 14+ τ10 9 14 13 – τ9 4 13 12	τring 4
71	S71=2τ14 13 12 11 – τ13 12 11 10 – τ12 11 10 9+2 τ11 10 9 4 – τ10 9 14 13 – τ9 4 13 12	τring 5
72	S72=τ13 12 11 10 – τ12 11 10 9 + τ109 14 13 – τ9 4 13 12.	τring 6
73	S73= γ10 9 8 21+ γ10 9 8 22	τC9C8
74	S74= γ15 1 8 21+ γ15 1 8 22	τN1C8
75	S75= γ15 1 2 3+ γ15 1 2 7	τN1C2

ISSN 2347-3487

Table 3: Assignments of fundamental vibrations of NBZA by normal coordinate analysis based n SQM force field calculations

Observed wave numbers (cm^{-1})		B3LYP/6-311**G(d,p) Calculated wave numbers(cm^{-1})	A_iIR^a	I_iR^b	Characterisation of normal modes with PED(%)
IR	Raman	Scaled			
3415(vs)	-	3415	20.3	110.7	υNH(100)
3077(w)	-	3069	5.3	244.1	υCH1(99)
3060(w)	-	3062	29.4	114.6	υCH1(99)
-	-	3060	16..4	334.2	υCH2(99)
3050(s)	3050(s)	3050	26.2	27.0	υCH2(99)
-	-	3045	23.3	100.7	υCH1(99)
-	-	3041	10.4	104.8	υCH2(99)
-	-	3036	1.7	104.5	υCH1(99)
-	-	3032	0.2	92.1	υCH2(99)
-	-	3027	4.9	27.0	υCH2(99)
3025(s)	3025(w)	3024	11.8	43.2	υCH1(99)
2923(s)	2927(m)	2927	20.2	67.7	CH_2AS(88),CH_2SS(12)
2846(m)	2846(w)	2846	48.4	131.3	CH_2SS(87),CH_2AS(13)
1582(w)	1582(w)	1582	142.0	115.2	υCC1(55),βCH(21), υCC2(10)
-	-	1579	52.6	6.5	υCC2(57), βCH(21), υCC1(10)
-	-	1565	0.6	12.4	υCC2(69), βCH(18)
1546(w)	-	1556	14.2	6.4	υCC1(63), βCH(16)
1489(s)	1492(w)	1497	245.4	11.3	βNH(27), βCH(26), υCC1(22), υCN(21)
-	-	1479	2.1	3.0	υCC2(55), βCH (22), υCC1(10)
-	-	1477	0.4	16.0	υCC1(43), βNH(20), βCH (14), υCC2(12)
1447(s)	1447(w)	1447	28.0	6.4	CH_2SC(88)
1431(s)	-	1437	10.1	1.0	υCC2(52), βCH(34)
-	1429(w)	1417	28.3	10.7	υCC1(43), βCH (28)
1360(m)	1361(w)	1363	0.8	4.6	CH_2WAG(66), βCH(12)
-	1333(w)	1313	44.5	7.8	βCH(69), υCN(13)
1321(s)	1319(w)	1312	27.8	3.0	βCH(73), υCN(11)
1300(s)	1302(w)	1306	65.9	16.0	υCC1(51), βCH(26), υCN(13)
1275(s)	1275(w)	1274	1.6	1.0	υCC2(80), βCH(11)
1249(w)	1246(w)	1230	19.4	0.8	βCH (65), υCC1(11)
-	1183(w)	1186	17.5	6.0	CH_2TWI(47), υCC2(17), βCH(10)
1179(s)	-	1174	2.7	28.9	βCH(26),CC_{ar}(21), υCC2(18),CH_2TWI(19), βR1(10)
-	1156(m)	1171	9.8	3.7	βCH(75), υCC1(17)
1151(s)	-	1168	0.3	6.9	βCH(71), υCC2(18)
-	-	1148	0.3	3.0	βCH(79), υCC2(20)

-	-	1145	2.1	5.5	βCH(83), υCC1(16)
1117(s)	1117(s)	1110	17.4	3.9	υCN(59)
1078(m)	1080(w)	1076	7.2	0.4	βCH (45), υCC2 (42)
1065(m)	1065(w)	1067	5.9	1.6	βCH (50), υCC1(34)
1026(m)	1028(m)	1025	8.7	10.3	υCC2(58), βCH(21)
-	-	1022	2.7	24.8	υCC1(71), βCH(22)
-	1000(s)	998	0.2	52.8	βR1(58), υCC2(41)
983(s)	987(s)	986	5.3	50.6	βR1(67), υCC1(29)
-	-	962	1.0	0.7	γCH2(81)
960(w)	-	960	4.0	3.4	CH_2RO(45), γ CH_2(20)
-	-	949	0.0	0.2	γ CH2(91)
-	-	945	0.0	0.3	γ CH(80)
-	-	930	0.0	0.22	γ CH(91)
904(w)	904(w)	902	6.4	5.3	γ CH2(69)
857(s)	866(w)	862	4.0	34.6	υCC1(22), γ CH2(19),CNC(13), βCCN(12)
-	-	843	3.9	0.3	γ CH(80)
827(w)	-	830	0.1	0.5	γ CH2(100)
794(w)	802(w)	794	0.5	0.6	γ CH(98)
-	784(m)	786	2.3	3.8	CC_{ar}(24),CC2(17),CC1(12), βR1(12), βR3(10), υCN(10)
734(s)	747(w)	738	31.2	3.5	γ CH2(40),τR1(35), τCC(13)
727(s)	-	725	66.0	1.3	γ CH(54), τR1(24), τCC(18)
695(s)	-	687	46.1	0.1	τR1(55), γ CH_2(38)
670(m)	-	674	20.3	0.3	τR1(67), γ CH(24)
626(w)	617(m)	619	2.0	3.1	βR2(58), τR1(10)
609(w)	-	604	0.5	3.5	βR2(70), βR3(15)
-	-	586	0.8	4.6	βR3(58), βR2(11)
526(w)	554(w)	533	33.4	1.1	CNC(20), τR2(12), τCC(11), γNH1(11)
506(s)	-	502	7.1	1.5	βR3(38), γNC(15), τR2(13)
486(w)	500(w)	501	9.9	0.2	γNC(27), τR2(25), γ CH(16), βR3(11)
457(w)	-	450	77.5	2.0	γNH1(24), γ $CH_2$1(20), τR2(12), γNH(12),CNC(12)
-	411(w)	411	0.0	0.1	τR3(61), τR2(19), γ CH(16)
-	-	406	3.0	0.2	τR3(64), γ CH_2(15), τR2(13)
-	343(w)	350	61.2	8.9	γNH1(28), γ $CH_2$1(20), γNH(18), βNC(16)
-	319(w)	321	1.1	1.1	βCC_a(56)
-	-	240	0.6	2.3	τR2(28), τR3(14), γ CH_2(11), βCCN(11)
-	-	226	0.7	0.7	τR2(42), τR3(16), γ CH(15), τR1(12)
-	178(s)	160	1.1	2.1	βNC(29),CNC(12), γCC(11)
-	110(s)	89	0.8	1.3	γNH(29), γNH1(25),CNC(18), γCC1(12)

-	82(s)	65	0.3	2.9	βCCN(28), γCC(27), γNH1(13)
-	-	36	0.1	4.6	γNH1(45), γNH(24)
-	-	22	0.1	9.5	γCC1(63), γ $CH_2$1(13), γCC(10)

vs –Very strong ; s – Strong; m- Medium; w – Weak; AS- Asymmetric; SS – Symmetric;

υ –Stretching; β - In plane bending; γ – out-of- plane bending; τ – Twisting:

4.4. Natural bond orbital (NBO) analysis

Natural Bond Orbital analysis provides an efficient analysis for studying intra and intermolecular bonding and interaction among bonds. It also provides a convenient basis for investigating charge transfer to conjugate interaction in molecular systems. The second - order Fock matrix has been carried out to evaluate the donor-acceptor interactions from NBO analysis [26].The interactions result in the loss of occupancy from the localized NBO of the idealized Lewis structure into an empty non Lewis orbital. For each donor (i) and acceptor(j) the stabilization energy E(2) associated with the delocalization i→j is determined as

$$E(2) = \Delta E_{ij} = q_i(F_{ij})^2/(E_j - E_i) \quad (2)$$

q_i is the donor orbital occupancy. E_i, E_j is the diagonal elements and F_{ij} is the off diagonal NBO Fock matrix element. The larger the stabilization energy E(2) value, the more intensive is the interaction between electron donors and electron acceptors.

Strong intramolecular hyper conjugative interactions (ICT) are formed by orbital overlap between LP(N1) and π*(C-C) bond orbital which result in ICT causing stabilization of the system. These interactions are observed as an increase in electron density (ED) in C-C antibonding orbital that weakens the respective bonds. The possibility of ED delocalization between the lone pair donor atom to antibonding acceptor atoms of the title molecule is shown in Table 4. It is evident from the Table, that the strongest electron transition is observed between the lone electron pair of N1 and neighbouring antibonding orbital of π*(C2-C7) which leads to a maximum stabilization energy of 33.18 $kcalmol^{-1}$. This is due to the fact that greater the value of E (2), the more intensive is the interaction between electron donors and acceptors. In NBZA, for the donor LP(N1), the occupancy is highly deviated from 2 and for the corresponding acceptor π*(C2-C7) there is an increase in occupancy(0.40788e). These results indicate a hyperconjugative interaction occurring between the donor LP(N1) and acceptor π*(C2-C7). The strong conjugation of electron - donating amino group with the π ring system leads to some changes of the bond lengths and bond angles of the aromatic ring.

In the title molecule, the intramolecular hyperconjugative interaction of σ(N1-H15), σ(C3-H16), σ(C4-H17), σ(C6-C7), σ(C7-H20), σ(C8-H21), σ(C10-H23), σ(C14-H27) distributes to σ*(C2-C7),σ*(C2-C3), σ*(N1-C2), σ*(C2-C3), σ*(C9-C14),σ*(C9-C10) respectively leading to a stabilization of ~4 $kcalmol^{-1}$.This enhanced NBO π (C2-C7) further conjugates with the antibonding orbitals of π*(C3-C4) and π*(C5-C6) which leads to a stronger delocalization of 16.21 and 24.04$kcalmol^{-1}$ respectively. The same kind of interactions have also been observed in the C3-C4 , C5-C6, C11-C12 and C13-C14 bonds as shown in Table 4.

Table 4 : Second order perturbation theory analysis of fock matrix in NBO basis for NBZA

Donor(i)	**ED(i)(e)**	**Acceptor (j)**	**ED (j) (e)**	**E (2) (kcal mol^{-1})**	**E(j)-E(i) (a.u)**	**F(i,j) (a.u)**
σ(N1-H15)	1.98186	σ*(C2-C7)	0.02466	4.14	1.20	0.063
		σ*(C2-C7)	0.02466	3.84	1.25	0.062
σ(C2-C7)	1.97095	σ*(C2-C3)	0.02197	3.83	1.25	0.062
π(C2-C7)	1.64479	π*(C3-C4)	0.33199	16.21	0.28	0.061
		π*(C5-C6)	0.35003	24.04	0.29	0.074
σ(C3-C4)	1.97785	σ*(N1-C2)	0.02547	3.65	1.15	0.058
π(C3-C4)	1.72193	π*(C2-C7)	0.40788	21.29	0.28	0.071
		π*(C5-C6)	0.35003	16.11	0.29	0.062
(σ C3-H16)	1.97809	σ*(C2-C7)	0.02466	4.45	1.08	0.062
		σ*(C4-C5)	0.01637	3.77	1.10	0.058
σ(C4-H17)	1.97979	σ*(C2-C3)	0.02197	4.01	1.07	0.059
		σ*(C5-C6)	0.01609	3.54	1.10	0.056
π(C5-C6)	1.68883	π*(C2-C7)	0.40788	16.53	0.28	0.062
		π*(C3-C4)	0.33199	22.68	0.28	0.071

σ(C5-H18)	1.98017	σ*(C3-C4)	0.01382	16.53	0.28	0.057
		σ*(C6-C7)	0.01431	22.68	0.28	0.058
σ(C6-C7)	1.97740	σ*(N1-C2)	0.02547	4.06	1.15	0.061
σ(C6-H19)	1.97976	σ*(C2-C7)	0.02466	3.98	1.07	0.058
		σ*(C4-C5)	0.01637	3.69	1.09	0.057
σ(C7-H20)	1.97781	σ*(C2-C3)	0.02197	4.19	1.08	0.060
		σ*(C5-C6)	0.01609	3.73	1.11	0.057
σ(C8-H21)	1.98465	σ*(C9-C14)	0.02531	4.42	1.08	0.062
π(C9-C10)	1.97422	π*(C13-C14)	0.31637	19.73	0.28	0.067
σ(C10-C11)	1.97834	σ*(C8-C9)	0.02032	3.74	1.12	0.058
σ(C10-H23)	1.97949	σ*(C9-C14)	0.02531	4.69	1.09	0.064
		σ*(C11-C12)	0.01620	3.64	1.10	0.057
π(C11-C12)	1.66923	π*(C9-C10)	0.34470	20.00	0.29	0.068
		π*(C13-C14)	0.31637	19.89	0,28	0.067
σ(C11-H24)	1.98043	σ*(C9-C10)	0.02338	3.72	1.10	0.057
		σ*(C12-C13)	0.01635	3.70	1.09	0.057
σ(C12-H25)	1.98030	σ*(C10-C11)	0.01551	3.81	1.09	0.058
		σ*(C13-C14)	0.01522	3.77	1.10	0.058
σ(C13-C14)	1.97846	σ*(C8-C9)	0.02032	3.60	1.12	0.057
π(C13-C14)	1.66721	π*(C9-C10)	0.34470	20.92	0.29	0.069
		π*(C11-C12)	0.32556	20.23	0.28	0.068
σ(C13-H26)	1.98049	σ*(C9-C14)	0.02531	3.75	1.09	0.057
		σ*(C11-C12)	0.01620	3.67	1.10	0.057
σ(C14-H27)	1.97897	σ*(C9-C10)	0.02338	4.68	1.09	0.064
		σ*(C12-C13)	0.01635	3.73	1.09	0.057
LP(1)N1	1.79439	π*(C2-C7)	0.40788	33.18	0.30	0.094
		σ*(C8-H21)	0.02919	7.65	0.65	0.066
		σ*(C8-H22)	0.02339	3.62	0.65	0.046

4.5. Frontier molecular orbital analysis

The most important frontier molecular orbitals (FMOs) such as highest occupied molecular orbital (HOMO) and lowest unoccupied molecular orbital (LUMO) play an important role in the chemical stability of the molecule[27].The HOMO represents the ability to donate an electron and LUMO as an electron acceptor represents the ability to accept an electron. The energy gap between HOMO and LUMO also determines the chemical reactivity and chemical hardness-softness of a molecule[28].The HOMO and LUMO energies are predicted at B3LYP method with 6-311++G(d, p) basis set. According to the results, the NBZA molecule contains 49 occupied molecular orbitals and 275 unoccupied virtual molecular orbitals. Fig. 5 shows the distributions of the HOMO-1, HOMO, LUMO and LUMO+1orbitals for the N-benzylaniline molecule. As seen from Fig. 5, in HOMO, the charge clouds are mainly located in aniline ring and methylene group. But the corresponding LUMO is mainly located in the benzyl ring. Consequently the HOMO-LUMO transition implies an electron density transfer from the aniline ring to benzyl ring. The HOMO-LUMO energy gap of NBZA has been calculated at the B3LYP/6-311++G(d,p) level. The calculated HOMO - LUMO gap energy shows that chemical hardness of the molecule.

$E_{HOMO(a.u)}$ =-0.19097 a.u.

$E_{LUMO(a.u)}$=-0.00882 a.u.

E_{HOMO}- E_{LUMO}(a.u)= 0.18215 a.u.

ISSN 2347-3487

4.6. Molecular electrostatic potential

The Molecular electrostatic potential (MESP) surface is plotted over the optimized electronic structure of NBZA using density functional B3LYP method with 6-311++G (d, p) basis set. The MEP generated in space around a molecule by the charge distribution is used to understand the reactive sites for nucleophilic and electrophilic attack in hydrogen bonding –interactions[29].The computationally observed MEP surface directly provides information about the electrophilic (electronegative charge region) and nucleophilic (positive charge region) regions.

The electrostatic potential at any point V(r) is the energy required to bring a single positive charge from infinity to that point. The electrostatic potential V(r) at any point in space around a molecule by charge distribution is given by

$$V(r) = \Sigma Z_A/|R_A-r| - \int \rho(r^l)dr^l/|r^l-r| \quad (3)$$

Where Z_A is the charge on the nucleus A, located at R_A and $\rho(r^l)$ is the electron density function of the molecule. To predict reactive sites for electrophilic (blue colour) and nucleophilic (red colour) regions MESP (Fig. 6) was carried out. As seen from the Fig. 6, there are two possible sites on the compound for electrophilic attack. The negative regions are mainly localized on the electronegative atoms. A maximum positive region is localized on the methylene group of the molecule and over the carbon atom C9 in the benzyl ring with a maximum value of 0.448 indicating a possible site for nucleophilic attack. The negative region is mainly over the aniline ring carbon atoms C3, C4, C5 with a maximum – 0.318.

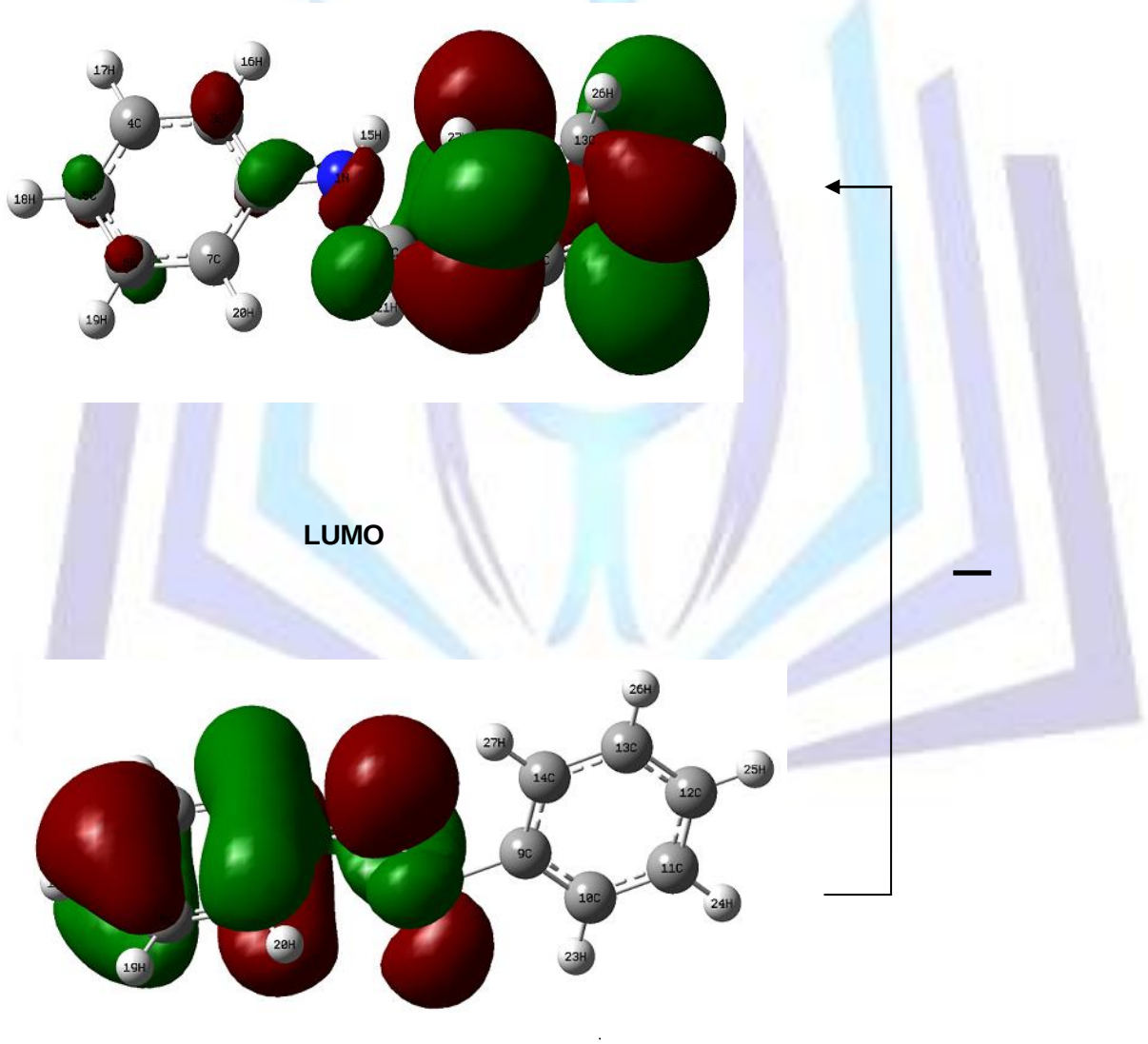

Fig. 5. HOMO and LUMO plot of N-benzylaniline.

ISSN 2347-3487

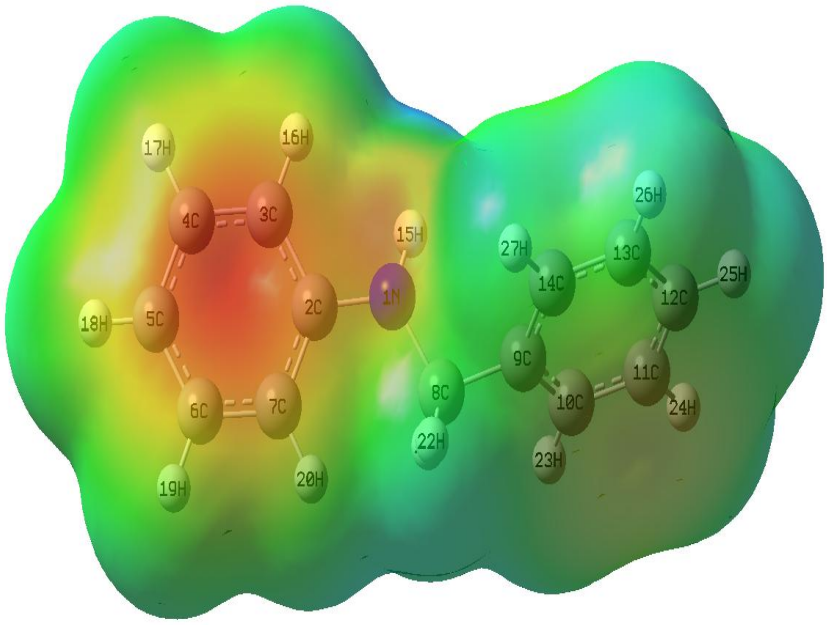

Fig 6: Molecular electrostatic potential map of NBZA calculated at B3LYP/6-311++G (d,p) level.

4.7. Thermodynamic properties

On the basis of vibrational analysis at B3LYP/6-311++G(d,p) level, the standard statistical thermodynamic functions: heat capacity(C) ,entropy(S) and enthalpy(ΔH) for the title compound were obtained from the theoretical harmonic frequencies listed in Table 6. From the table, it can be observed that these thermodynamic functions are increasing with temperature ranging from 100 to 1000K due to the fact that molecular vibrational intensities increase with temperature [30].The values of some thermodynamic properties such as thermal energy, vibrational energy, zero-point vibrational energy, rotational constants and dipole moment of NBZA by B3LYP/6-311++G(d,p) method are listed in Table 7.

The correlation equations between heat capacity, entropies, enthalpy changes and temperatures were fitted by quadratic formulas using the corresponding fitting factor (R^2). The corresponding fitting equations are as follows and the correlation graphs are shown in Fig. 7.

$C = -2.0249 + 0.19662\ T - 7.67295 \times 10^{-5} T^2$ ($R^2 = 0.99815$)

$S = 59.27139 + 0.1826\ T - 2.992462 \times 10^{-5} T^2$ ($R^2 = 0.99993$)

$H = -1.59681 + 0.01672\ T - 5.70513 \times 10^{-5} T^2$ ($R^2 = 0.99946$)

4.8. Mulliken atomic charges

The charge distribution of the molecule is calculated on the basis of the Mulliken method [31] using B3LYP/6-311++G(d,p) level calculation. This calculation depicts the charges of every atom in the molecule. The distribution of positive and negative charges is vital to the variation of bond length between the atoms. Atomic charge affects dipole moment, polarizability, electronic structure and other molecular properties of the system. Atomic charges of the title compound computed by mulliken method are presented in Table8.

In Table 8, it is observed that all the hydrogen atoms have a net positive charge. The positive charge of the H atom in the N-H group is found to possess a high atomic charge. This is due to the attachment of highly electronegative nitrogen atom. The magnitudes of the carbon atomic charges for the compound are found to be both positive and negative. The negative values on C2,C3,C4,C5 and C6 atoms in the aniline ring and C8,C10,C11,C12,C13 and C14 atoms in the benzyl ring lead to redistribution of electron density.

ISSN 2347-3487

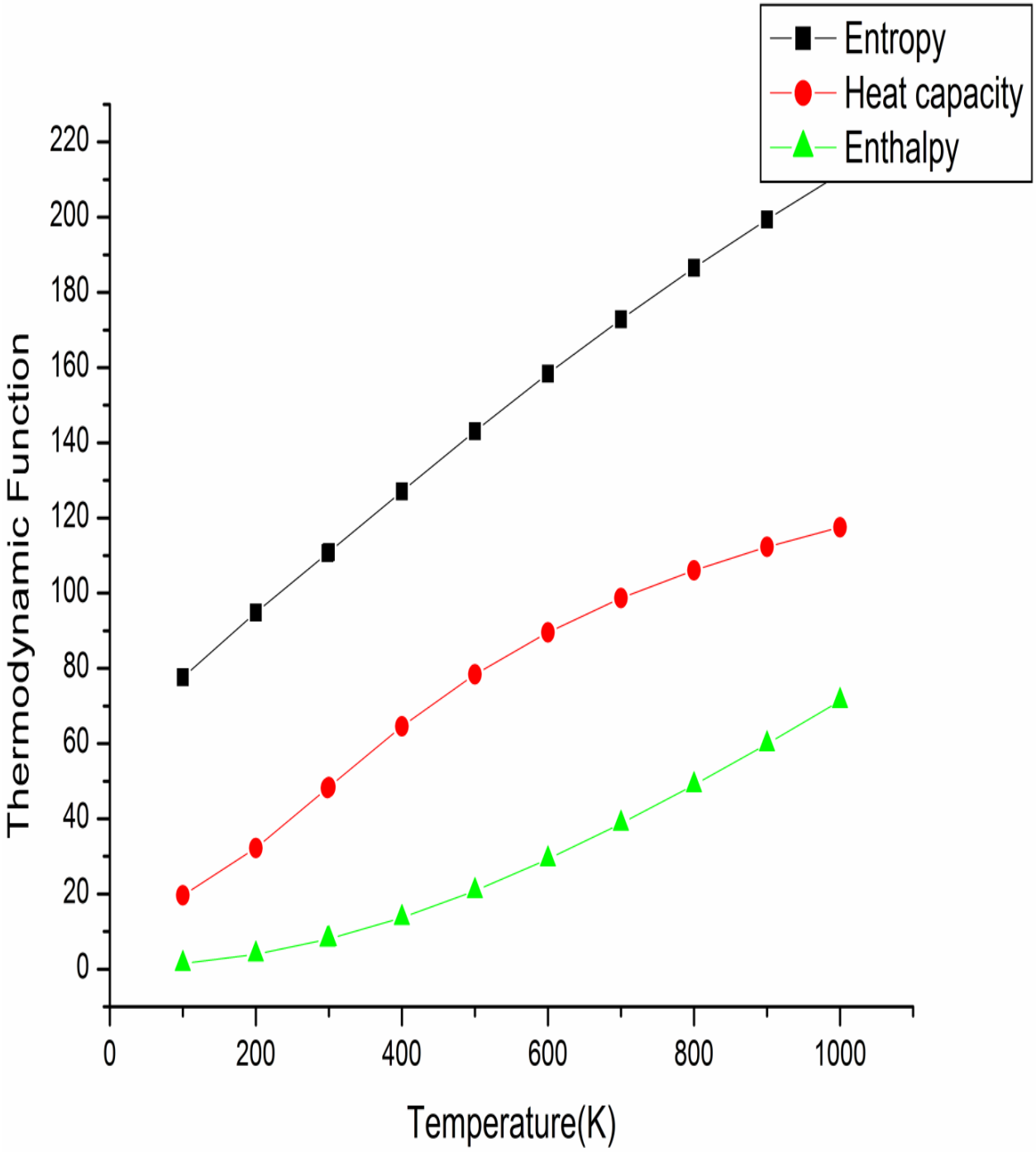

Fig.7: Correlation graph of thermodynamic function (entropy, heat capacity and enthalpy) and temperature for N – benzylaniline.

4.9. UV-Vis analysis

The electronic absorption spectra of NBZA compound were recorded in the polar solvents ethanol and water as displayed in Fig. 8. The observed λ_{max} in ethanol and water are 246nm and 238nm respectively. The peaks arise mainly because of n→π* transition. Due to When NH_2 group is attached to benzene ring, its absorption changes from λ_{max}(255nm) to λ_{max}(280nm) [32]. But in the title compound, the λ_{max} is blue shifted both in the solvents water and ethanol due to the attachment of benzyl ring with the aniline ring. From HOMO LUMO analysis, HOMO is existed on the aniline ring and the LUMO is residing on the benzyl ring. Hence, HOMO → LUMO transition is due to the excitation of electrons from LP(N) to π* orbitals of benzyl ring. This could also be verified in NBO analysis by the large delocalization of n→π* transition (Table. 4)

ISSN 2347-3487

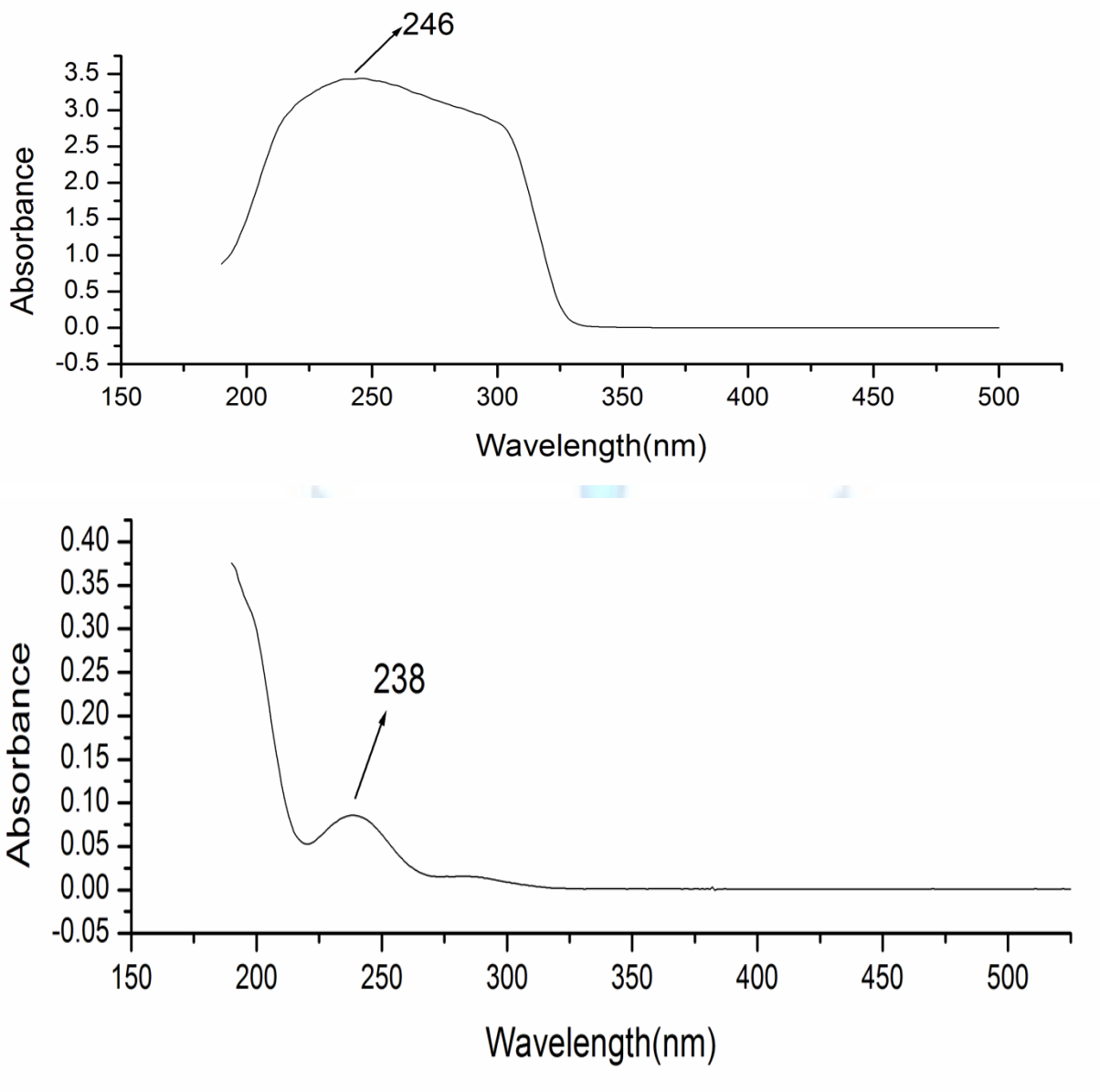

Fig.8. UV – vis absorption spectrum of NBZA in ethanol and water solvents.

5. Conclusion

DFT studies of N- benzylaniline molecule were performed to obtain the detailed vibrational properties and other structural properties at B3LYP/6-311++G (d, p) level of theory. The geometrical structural analysis shows that the calculated bond lengths and bond angles are in good agreement with the experimental values. Substitution of NH_2 and methylene groups distorts the molecular geometry. Four local global minimum were observed at the dihedral angles 30^0, 180^0, 200^0 and 350^s for τ(C8-N1-C2-C3) in potential energy surface scan analysis. The vibrational spectra of the compound were recorded, and on the basis of experimental results and PED calculations, assignments were given for all the fundamental vibrational frequencies. From the NBO analysis, the hyperconjugative interactions were observed from the amino group LP (N) atom to aromatic π*(C2-C7) and it leads to the change in bond lengths and bond angles. From the HOMO-LUMO analysis the effective charge transfer from aniline to the benzyl ring was observed in pictorial format. The Molecular electrostatic potential analysis revealed the two possible electrophilic and nucleophilic attacks aniline ring and methylene group respectively. The increasing of thermodynamic functions with temperature was established in thermodynamic property analysis. Mulliken atomic charges were analysed for the substitution effect in the molecule. The UV-Vis analysis indicates the substituent effect of amino group by the shift of the maximum absorption band.

6. ACKNOWLEDGEMENT

The authors are thankful to Sophisticated Analytical Instrumentation Faculty (SAIF), IIT Chennai for the spectral measurements.

7. REFERENCES

[1] L. J. Bellamy, B.I. Williams, Spectrochim. Acta. 9. 341 – 345 9 (1957).

[2] M. A. V. Ribeiro da silva, A. I.M.C.L. Ferreira, J.R.B. Gomes, J. Phys. Chem.

B111. 2052 – 2061 (2007).

[3] A. Heaton, M. Hill, F. Drakesmith, J. Fluorine, chem. 81. 133-138 (1997).

[4] V. Krishnakumar, V. Balachandran, Spectrochim.Acta A .61. 1811-1819 (2005).

[5] N. Sundaraganesan, M. Priya, C. Meganathan, B. Dominic Joshua, J. P. Cornard, Spectrochim.Acta. A. 70. 50 – 59 (2008).

[6] Patentscope.Wipo.int.

[7] M. J. Frisch et al., GAUSSIAN 03 Program, Gaussian, Inc.,Wattingford. CT.2004.

[8] G. Rauhut. P. Pulay, J. Phys. Chem. 99. 3093 – 3100 (1995).

[9] P. Pulay. G. Fogarasi. G. Pongoe. J. E. Boggs. A, Vargha. J. Am. Chem. Soc. 105. 7037 – 7047 (1983).

[10] G. Fogarasi, P. Pulay. J. R. Durig (Eds.), Vibrational Spectra and structure. Vol. 14.ElsevierPublications. Amsterdam. 1985.

[11] G. Fogarasi. N. Zhov. P. W. Taylor. P. Pulay. J. Am. Chem. Soc. 114. 8191 – 8201 (1992).

[12] T. Sundius, J. Mol. Struct. 218. 321 – 326 (1990).

[13] T. Sundius, vib. Spectrosc.29. 89–95 (2002).

[14] G. keresztury, S. Holly. J. Varga, G. Besenyei, A. Y. Wang, J. R. Durig, Spectrochim.Acta .A. 49. 2007 – 2017 (1993).

[15] G. keresztury, in : J. M. Chalmers, P. R. Griffith (Eds.), Raman Spectroscopy: Theory ,Handbook of Vibrational Spectroscopy, Vol. 1 John Wiley and Sons Ltd. New York, 71 – 87 (2002).

[16] E. D. Glendening. A. E. Reed, J. E. Carpenter, F. Weinhold, NBO Version 3.1. TCI,University of Wisconsin, Medison, 1998.

[17]R.Betz, C.McCleland, H.Marchand, Actacrys. E. 67 o1195 (2011).

[18] P.Gayathri, J. Jayabharathi, G. Rajarajan, A. Thiruvalluvar, R. J. Butcher. Actacrys.E. 65 o3083 (2009).

[19] M.V.S.Prasad, KadaliChaitanya, N.Udaya Sri, V.Veeraiah, Spectrochim. Acta. A. 99. 379-389 (2012).

[20] S. Ramalingam, S. Periandy, B. Narayanan, S. Mohan, Spectrochim. Acta. A. 76. 84 – 92 (2010).

[21] Y. Wang, S. Saebar, C. U. Pittman, J. Mol. Struct. (Theochem) 281. 91 – 98 (1993).

[22]A.Altun, K.Golcuk, M.Kumru, J. Mol. Struct. (Theochem) 637.155 – 169 (2003).

[23] N.P.G.Roeges, A Guide to complete Interpretation of Infrared Spectra of Organic Structures, Wiley, New York, 1954

[24] G.Varsanyi ,Assignments for Vibrational spectra of seven hundred Benzene Derivatives, vol. 12. Adam Hilger, 1974.

[25] G. Socrates, Infrared Raman Charateristic Frequencies, 3rd ed.. John Wiley & Sons Ltd, Chichester, 2001

[26] M.Szafran, A.Komasa, E.B.Adamska, J. Mol. Struct.(Theochem)827. 101 – 107 (2007).

[27] S. Gunasekaran, R.A.Balaji, S.Kumaresan, G.Anand, S.Srinivasan, Can. J. Anal. Sci. Spectrosc. 53. 149–160 (2008).

[28] B.Kosar,C.Albayrak,Spectrochim. Acta. A. 78. 160 – 167 (2011).

[29] R.G.Pearson,Proc.Natl.Acad.Sci.83. 8440 – 8441 (1986).

[30]J. Bevanott, Calculations from Statistical Thermodynamics, Academic Press, 2000.

[31] I. Sidir, Y.G. Sidir, M. Kumalar, E. Tasal, J. Mol.Struct. 964. 134 – 138 (2010).

[32] Y.R.Sharma, Elementary organic spectroscopy, S.Chand& Company Ltd. 2001